Proceedings ICFDP7:
7TH International Congress on Fluid Dynamics and Propulsion
Dec. 18-20, 2001, Cairo, EGYPT

ICFDP7-2001050

SPRAY CHARACTERISTICS OF TWO PHASE SWIRL ATOMIZER

Byung-Joon Rho
Prof., Faculty of Mechanical & Aerospace Engrg.,
Chonbuk National University & RIIT, Korea

Sam Goo Lee
Research Fellow, AHTRI, Chonbuk National University, Korea

Kyu-Keun Song
Prof., Faculty of Mechanical & Aerospace Engrg.,
Chonbuk National University & AHTRI, Korea

Jae-Youn Jung
Prof., Faculty of Mechanical & Aerospace Engrg.,
Chonbuk National University & TIC, Korea

ABSTRACT

The experimental measurements were carried out to examine turbulent disintegration characteristics ejecting from the counter-flowing internal mixing pneumatic nozzle under the different conditions such as swirl angles and air pressures. The air injection pressure was varied from 60 kPa to 180 kPa and four counter-flowing internal mixing nozzle with axi-symmetric tangential-drilled four holes at swirl angle of 15°, 30°, 45°, and 60° to the central axis has been specially designed. The experimental results are quantitatively analyzed, focusing mainly on the comparison of turbulent atomization characteristics issuing from an internal mixing swirl nozzle. To illustrate the swirl phenomena, the distributions of mean velocities, turbulence intensities, volume flux, and SMD (Sauter Mean Diameter, or D_{32}) are comparatively analyzed.

INTRODUCTION

The disintegration mechanism in twin fluid atomizers is still being investigated in order to characterize the optimum models. Regarding this consideration, one of the prerequisites for the good atomization is to get a high momentum of the droplets, caused by the mutual interactions. The purpose of breaking up the liquid into multitudinous small droplets is to increase the liquid surface area and to improve the disintegration. That is, the atomization in two-phase flows is most effectively achieved by generating a high relative velocity between the liquid jet and the surrounding air. Also, air to liquid mass flow ratio (ALR) and geometric configuration of the nozzle are known as important parameters affecting the mixing process. In this article, nozzle configurations were varied within the passages of twin fluids.

A large number of literatures have been reported on the disintegration process, and some improved results were obtained. A Mansour et al.[1] and S.G. Lee et al.[2] showed that the SMD is progressively reduced as the ALR is increased. J. B. Kennedy [3] found that the SMD changed linearly with the surface tension while the influence of the viscosity was minimized. S. G. Lee [4,5] showed the results that the smaller droplets are inwardly entrained from the spray boundary. Mullinger and Chigier [6] showed the advantage for the internal mixing atomizers that the atomizing fluid can generally be supplied to the mixing region at a higher pressure than the external mixing type.

The aim in this experimental investigation was intended to describe the turbulent mixing flow and disintegration characteristics issuing from the internal mixing counterflowing two-phase jets.

NOMENCLATURE

d_o: Final discharge orifice diameter
d_p: Diameter of passages for the fluids
D_s: Swirl chamber diameter
l_o: Length of final discharge orifice
l_s: Length of swirl chamber
l_{ap}: Length of air passages
l_{wp}: Length of liquid passages
q_s: Swirl angle of the inlet passages for the fluids
ALR: Air to liquid mass ratio
D_{32}: Sauter mean diameter
R: Radial distances
U_m: Maximum axial velocity at the centerline
u'_{rms}: Root mean square in axial velocity
U: Axial velocity
V: Radial velocity
W: Tangential velocity
Z: Axial distances from the nozzle tip

EXPERIMENTAL METHODOLOGY

Nozzle

The body of prototype nozzle for generating a counter-flowing spray was fabricated of brass, and the nozzle configuration is schematically shown in Fig. 1. The discharge orifice diameter (d_o) is 2mm, swirl chamber diameter (D_s) is 9mm, and the length to diameter ratio of the discharge orifice is 0.65 ($l_o \approx$ 1.3mm). The working fluids were inflowed through the tangential ports that generated the liquid and the air an angular velocity, interacted together in the mixing chamber and injected into the quiescent ambient air at room temperature.

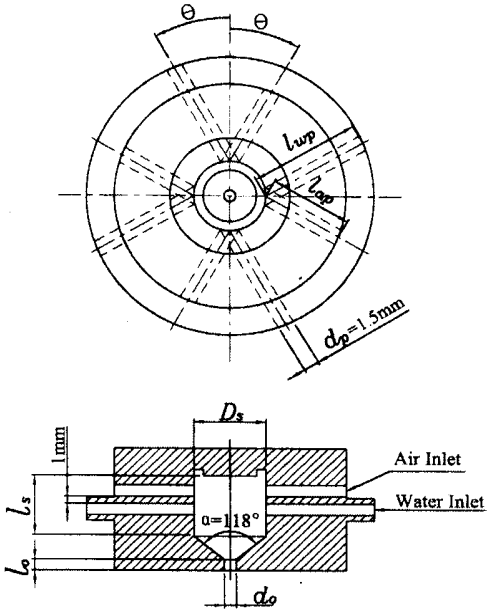

Fig.1 Geometric nozzle configuration used for the experiment

Experimental Set-up

The experimental apparatus is shown schematically in Fig.2. Continuous and steady flowing water and the pulsation-free air are supplied to the mixing chamber from the pressurized storage tank. Working fluids were properly filtered and regulated. A number of valves, pressure gauges, and flow meters are set up to control the flow rates. Experiments were conducted for the liquid flow rate was kept constant at 7.95 g/s and the air pressures were gradually increased from 20 kPa to 200 kPa, and ALR can be varied from 0.054 to 0.132.

PDPA Systems

Phase Doppler Particle Anemometer was installed to measure the droplet's behavior of the spray. It provides information on individual particle size between 1 μm and 250 μm passing through the measurement volume in this investigation. The focal lengths of the transmitting and receiving optics were 400mm and 500mm, respectively. The photo-muitiplier detector voltage of 1400V was optimized to provide the greatest sensitivity, and 45° of scattering was made in the forward direction. Also, bragg cell was used to shift the frequency of one beam by 40 MHz to provide directional sensitivity. Data acceptance rate in this experiment was too low for distances less than 20 mm from the nozzle exit. Reasons for the low S/N ratio was usually attributed to the presence of non-spherical particles in the PDPA probe volume. Because the PDPA works on the principle of light scattering by spherical particles, signals from non-spherical particles will reject by the instrument. Data acceptance rate varied from 60% to 98% depending on the experimental conditions and the location of the probe volume in relation to the spray geometry.

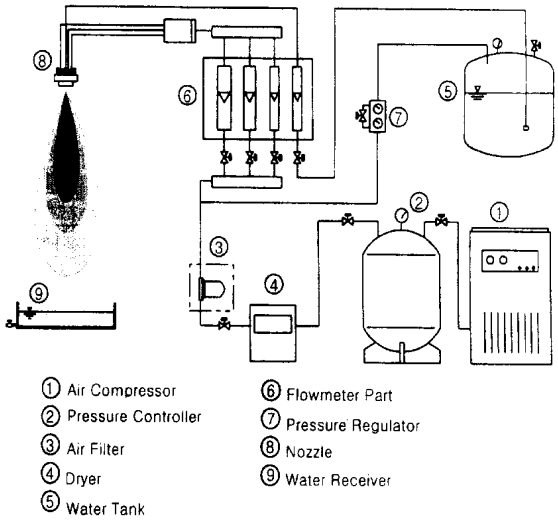

Fig.2 Schematic set-up for the experimental apparatus

Coordinate System

Radial profiles of a geometric sequence space at each measurement locations were obtained at 6 axial positions downstream from the nozzle exit, respectively. The coordinate Z corresponds to the downstream direction at the nozzle exit and y signifies radially outward motion. The measurement volume can be positioned easily at various stations without moving the diagnostic systems in three orthogonal directions by using a computer controlled traversing system that permits positioning to within 0.02 mm.

Data Acquisition

The droplet quantities were calculated by collecting 10,000 sample data at each point. The sampling time depends on the local number density of drops, and the 10 sec. was set as the upper limit to record data. Precautions for the accurate measurement were taken to avoid possible sources of error during the experiments such as mistracking the particles,

nozzle vibrations, and the reading of the flow meters, etc.. Also, the mists of small droplets were discharged to an exhaust system to prevent splashing. To establish the repeatability of the data received, each profile was measured at least twice at different times.

RESULTS AND DISCUSSION

Fig.3 indicates a characteristic sequence of the liquid jet structure based on photographs at different conditions. The liquid from the nozzle emerges as less disintegrated jet at lower ALR as shown in Fig. 3a. The tangential swirling motion at the exit orifice is noticeable as the swirl angle increases.

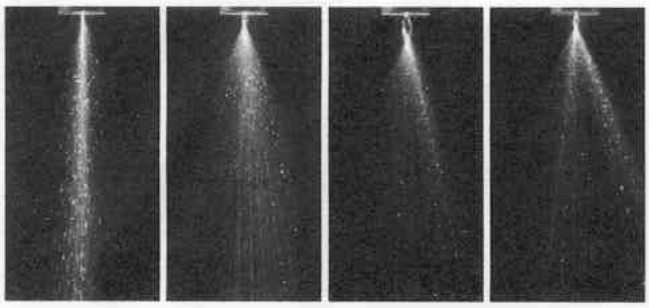

Fig. 3a Photographic visualization for the lower ALR

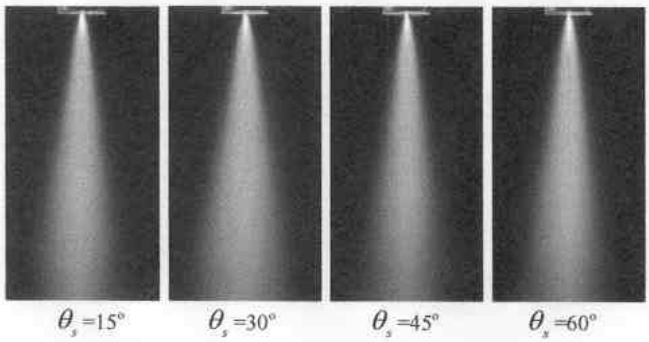

Fig. 3b Photographic visualization for the higher ALR

At the beginning stage, the swirl impacts can be seen evidently, and the liquid emerges as a twisting conical sheet as shown in Fig. 3a. But, at some distances away from the nozzle tip, some ripples appear and grow, indicating the typical aspect of the swirl atomizer. Thus, it can explain the breakup process, corresponding to the contraction due to the drag, and the dispersion by the swirl, which finally cause the discontinuities of droplets issuing from the atomizer. That is, the twisting bubble shape of converging sheet abruptly diverges, leading to the disintegration into filaments and large drops even for the lower ALR case.

On the other hand, with the higher air mass ratio as shown in in Fig. 3b, no perturbations appear and the number of clusters was remarkably reduced compared to the Fig. 3a. Also, the breakup region gradually moves back close to the nozzle with the increase of air mass rate and the twisting onion shape can't be seen any more. Fig. 3b was increased the air mass flow rate by a factor of three relative to the flows in Fig.3a. It indicates an increase of radial expansion so that disintegration aspects were more readily observed. That is, an increase in the air mass flow rate resulted in an increase for the spray angle and the smaller droplets.

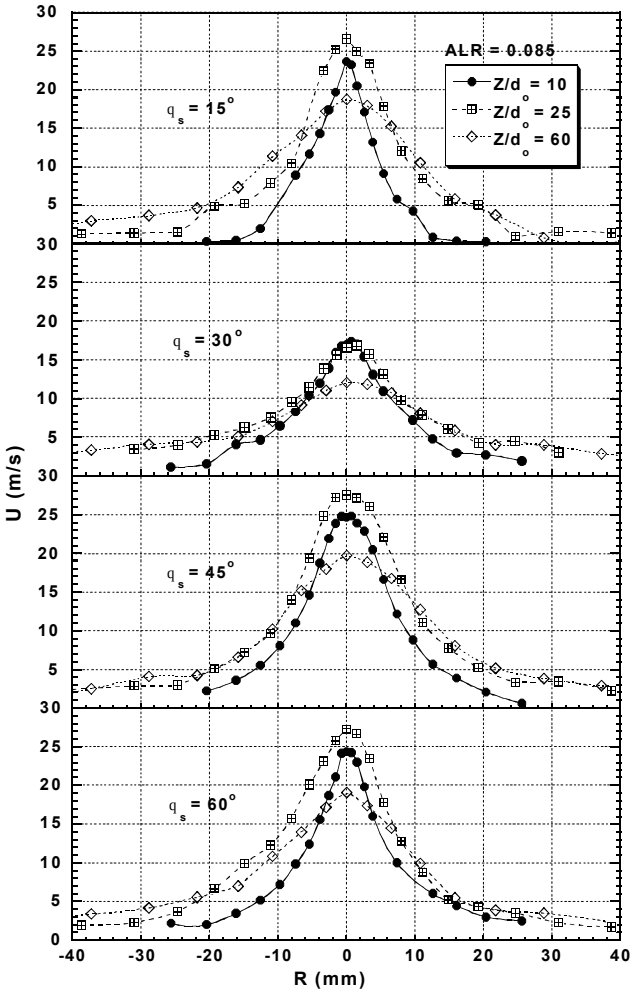

Fig.4 Distributions of axial mean velocity for different swirl angles measured at three axial downstream locations

Fig.4 shows the radial profiles of mean axial velocity at three axial positions under the different swirl angles. It is considered that the droplets emanating from the nozzle exhibit an explicit flow similarity regardless of different swirl angles. It also reveals the droplet in the central parts propagate farther downstream due to easy access of atomizing air, whereas the

accelerations at the spray boundary are discernibly less by the loss of axial momentum and the surrounding drag. This is attributed to the fact that the spray behavior near the axis seems to have higher momentum and is subject to higher acceleration even though its geometric conditions are dissimilar. Although the distributions are seen to be geometrically symmetric about the spray axis, and they have nearly qualitatively consistent value when compared, the effects of swirl inclination for q_s =30^o are quite visible. The distributions for the case of q_s =30^o are much smaller even in the central parts. This difference in velocity variation can be possibly substantiated by the photographic observation in Fig.3. The spray dispersion is wider than those of other angles. This growth rate because of the swirling characteristics in case of q_s =30^o hinders the axial downward propagation.

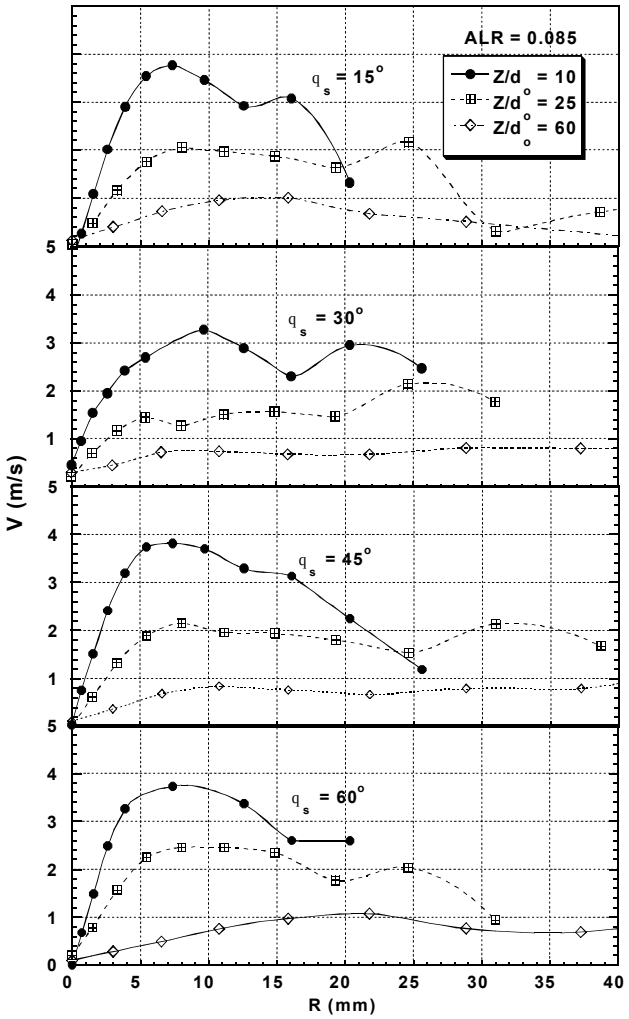

Fig.5 Distributions of radial mean velocity for different swirl angles measured at three axial downstream locations

The distributions in Figs. 5-6 indicate another significant characteristic feature of swirling atomizer. The radial and tangential velocities in the center show a minimum value, which comprise the maximum in axial velocity as shown in Fig.4. This is mainly because the effects of downward axial penetration tend to subside the growth rate. But the spray trajectory in radial and tangential components exhibit a progressive dispersion to the outer, shifting the location of maximum velocity at all conditions. After reaching a maximum value, the velocities are sluggishly decreased. Even though the spray patterns are similar, big differences in velocity are apparent between two components.

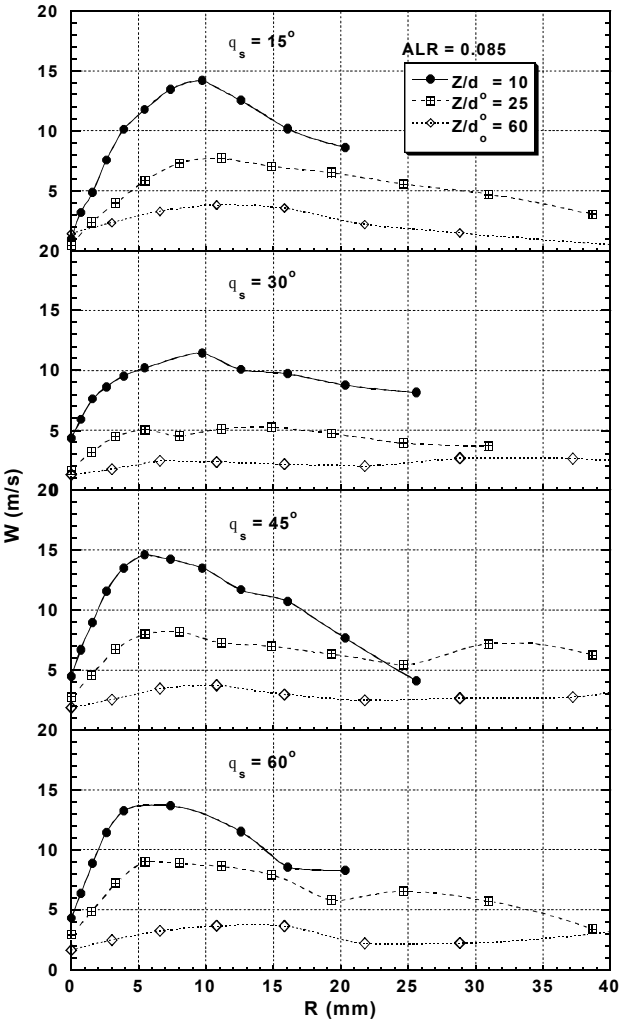

Fig.6 Distributions of tangential mean velocity for different swirl angles measured at three axial downstream locations

The spray transport is quite comparable as indicated by the turbulence intensities in Fig.7. The droplets located in the center and the downstream regions have the maximum axial turbulence intensity in all conditions, while having comparatively smaller values toward the boundary and

upstream locations.

This explains that the sprays acquire large velocity fluctuations for all the cases in the center as an acceleration stage. But, an interesting result can be drawn from this. Even with a higher axial momentum close to the nozzle exit, the downstream turbulence intensities are much higher than the upstream. This is presumably caused by the non-spherical particles or less disintegrated droplets at upstream. As the sprays are in the developing process, it is considered that the better atomization of the droplets could be observed at downstream region, which is one of the characteristics in counter-swirling internal mixing nozzle.

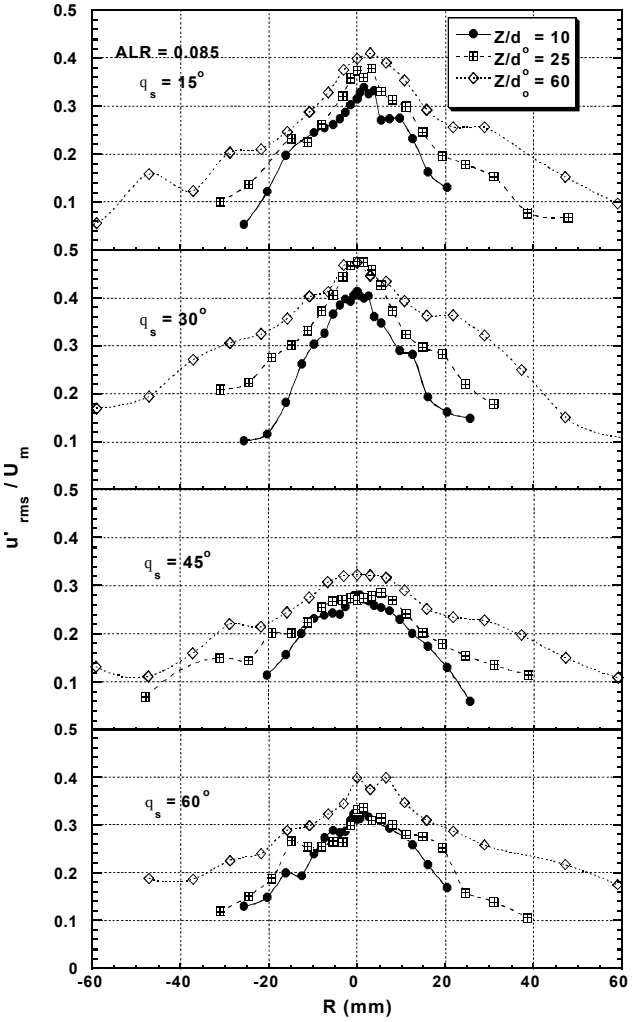

Fig.7 Distributions of turbulence intensities for different swirl angles measured at three axial downstream locations

Fig.8 shows the SMD variation measured at different swirling angles. At upstream regions, the droplets even in the center part are typically larger than that of the downstream. As shown for all the cases, the initial increase in SMD is due

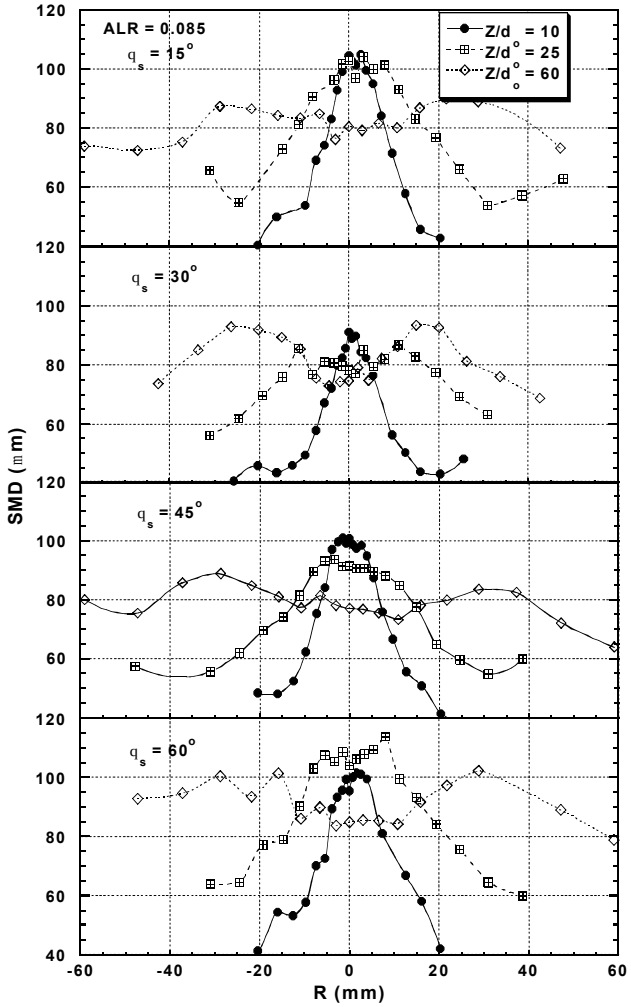

Fig.8 Distributions of Sauter mean diameter for different swirl angles measured at three axial downstream locations

to the possibility of coalescence from the less atomized droplets in spite of strong penetration, showing that SMD decreases from approximately 80-110 at upstream to 60-90 at downstream. Contrast to the upstream transport, however, the SMD in the spray periphery gradually increases, which might be explained by the entrainment of small droplets from the outer part to the central region. This result was reported in the previous research that the smaller droplets in the peripheral region tend to be entrained inwardly and the larger ones inclined to remain in the region. The smaller droplets at upstream are less abundant in the center region, and the presence of relatively smaller ones near the boundary is ascribed to the distinctive feature in this swirl nozzle. Also, it is interesting to observe that the variation in SMD for q_s=30° is the lowest among these nozzles. It could be substantiated by the photographic pattern as shown in Fig.3. It is also confirmed that the wider radial growth rate restrains the axial penetration and the brisk turbulence fluctuation means better

atomization in the spray field.

Distributions of volume flux in Fig.9 show a good coincidence with the SMD variation as shown in Fig.8. At upstream, the high rates of volume fluxes are existed on the axis, but the trend for the downstream is quite different. The examination of these profiles provides a discernible difference for q_s =30°. The volume fluxes in this angle are evidently smaller than those of the other swirl angles, indicating more positive influence on the improved atomization. The highest volume flux near the spray boundary at all conditions means the dense concentration of comparatively higher number density with larger drop diameters.

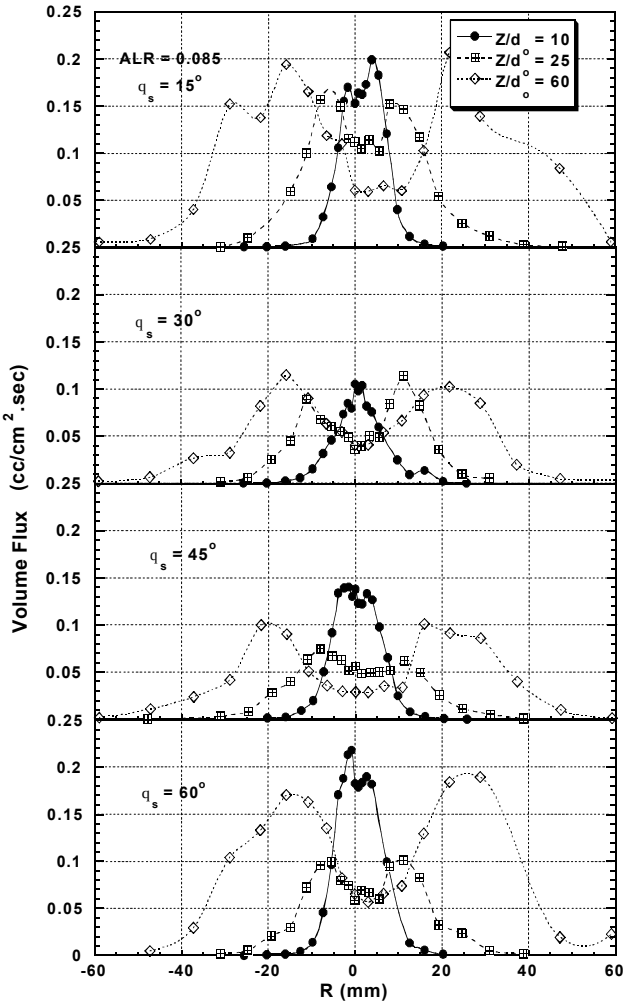

Fig.9 Distributions of volume flux for different swirl angles measured at three axial downstream locations

CONCLUSIONS

From the experimental analysis for the internal mixing swirl spray, the following conclusions can be drawn.

Photographic visualization shows that no twisting conical perturbations for the higher ALR can be seen as they did for the case of the lower ALR. It indicates that an increase of ALR resulted in an expansion of radial growth rate, reducing the number of clusters. Although the axial velocity distributions for q_s =30° are much smaller even in the central parts, it can explain the positive swirl effects for disintegration. Especially, the turbulence intensities for the case of q_s =30° are higher than the other cases at all axial locations, explaining brisk velocity fluctuations with higher swirl momentum. As indicated for all the variations in SMD and volume flux, the initial increase is due to the possibility of coalescence of the less disintegrated droplets with dense concentration. Thus, the nozzle configuration with a swirl angle of 30° to the central axis is recommendable for better disintegration compared to the other ones.

ACKNOWLEDGEMENTS

This work was supported by the Research Institute of Industrial Technology at Chonbuk National University

REFERENCES

1. Adel Mansour and Norman Cgigier, 1990, "Disintegration of liquid sheets", Phys. Fluids A., pp. 706-719
2. S.G. Lee, K.C. Kim, J.H. Namkung, B.J. Rho, and K.K. Song, 2001, "Spray Transport and Atomization in two phase swirl atomizer", Proceedings of ILASS-Asia 2001
3. J. B. Kennedy, 1986, "High number SMD Correlations for pressure atomizers", Journal of Engrg., for Gas Turbines and Power. pp. 191-195
4. S. G. Lee and B. J. Rho, 2000, "Atomization characteristics in pneumatic counterflowing internal mixing nozzle." KSME International Journal, Vol. 14, No. 10, pp. 1131-1142
5. S. G. Lee, B. J. Rho and K. K. Song, 2001, "Turbulent disintegration characteristics in twin fluid counter flowing atomizer." 39th ALAA Aerospace and Sciences Meeting and Exhibit, AIAA 2001-1047, Reno Nevada
6. P. J. Mullinger, 1974, "The design and performance of internal mixing multijet twin fluid atomizers", Journal of the Institute of Fuel. pp. 251-261